Tellus SERIES B CHEMICAL AND PHYSICAL METEOROLOGY
PUBLISHED BY THE INTERNATIONAL METEOROLOGICAL INSTITUTE IN STOCKHOLM

Climate warming and decreasing total column ozone over the Tibetan Plateau during winter and spring

By JIANKAI ZHANG[1], WENSHOU TIAN[1]*, FEI XIE[2], HONGYING TIAN[1], JIALI LUO[1], JIE ZHANG[1], WEI LIU[1] and SANDIP DHOMSE[3], [1]*Key Laboratory for Semi-Arid Climate Change of the Ministry of Education, College of Atmospheric Sciences, Lanzhou University, Lanzhou, China;* [2]*State Key Laboratory of Numerical Modeling for Atmospheric Sciences and Geophysical Fluid Dynamics, Institute of Atmospheric Physics, Chinese Academy of Sciences, Beijing, China;* [3]*School of Earth and Environment, University of Leeds, Leeds, UK*

(Manuscript received 22 November 2013; in final form 1 April 2014)

ABSTRACT

The long-term trends of the total column ozone (TCO) over the Tibetan Plateau (TP) and factors responsible for the trends are analysed in this study using various observations and a chemistry–climate model (CCM). The results indicate that the total column ozone low (TOL) over the TP during winter and spring is deepening over the recent decade, which is opposite to the recovery signal in annual mean TCO over the TP after mid-1990s. The TOL intensity is increasing at a rate of 1.4 DU/decade and the TOL area is extending with 50,000 km^2/decade during winter for the period 1979–2009. The enhanced transport of ozone-poor air into the stratosphere and elevated tropopause due to the rapid and significant warming over the TP during winter reduce ozone concentrations in the upper troposphere and lower stratosphere and hence lead to the deepening of the TOL. Based on the analysis of the multiple regression model, the thermal dynamical processes associated with the TP warming accounts for more than 50% of TCO decline during winter for the period 1979–2009. The solar variations during 1995–2009 further enlarge ozone decreases over the TP in the past decade. According to the CCM simulations, the increases in NOx emissions in East Asia and global tropospheric N_2O mixing ratio for the period 1979–2009 contribute to no more than 20% reductions in TCO during this period.

Keywords: total column ozone, Tibetan Plateau, climate warming, nitrous oxide

1. Introduction

Due to its strong ultraviolet absorption and greenhouse effect, ozone plays an important role in the atmospheric radiation balance (Forster and Shine, 1997). As a result of human activities, global total column ozone (TCO) has decreased remarkably over past decades. However, since the signing of the Montreal Protocol in 1987, some chlorofluorocarbons (CFCs) and other ozone-depleting substances (ODSs) in the atmosphere are decreasing steadily, and the stratospheric ozone is expected to recover in the future (WMO, 2011). Recent chemistry–climate model simulations indicate that the recovery of ozone over the lower latitudes is different from that over higher latitudes (Austin et al., 2010).

The Tibetan Plateau (TP), the highest topography in the world, not only has a significant impact on the atmospheric circulation and climate system in East Asia (e.g. Yanai et al., 1992; Ye and Wu, 1998) but also has a remarkable influence on the ozone distribution (e.g. Tian et al., 2008). Under the situation of global ozone recovery and climate changes, whether the ozone over the TP exhibits trends similar to those over other regions of the earth is a question worth investigating. Zhou et al. (1995) found from the Total Ozone Mapping Spectrometer (TOMS) satellite measurements that there is a remarkable low TCO centre over the TP in the summer, which is called as the 'ozone valley'. This phenomenon was also found in ozonesonde observations at Lhasa station of the TP (Tobo et al., 2008). A question arises as to whether the so-called 'ozone valley' over the TP is recovering or deepening.

Although the mechanisms for the formation of low TCO centre over the TP have been researched in previous

*Corresponding author.
email: wstian@lzu.edu.cn
Responsible Editor: Annica Ekman, Stockholm University, Sweden.

Citation: Tellus B 2014, **66**, 23415, http://dx.doi.org/10.3402/tellusb.v66.23415

studies (e.g. Zou, 1996; Ye and Xu, 2003; Zheng et al., 2004; Tian et al., 2008), less attention was paid to the ozone trend over the TP due to the lack of long-term observations. Ye and Xu (2003) analysed the TOMS data from 1979 to 2000 and reported that the interannual variability of annual mean TCO over the TP is in phase with but weaker than the plateau's corresponding zonal mean TCO. They also argued that the interannual variability of TCO over the TP is controlled by a mechanism with a scale much larger than the topography of the TP. It is known that global ozone abundance and its trend are mainly controlled by the ODSs in the atmosphere and atmospheric conditions. The relative importance of physical and chemical processes influencing the variability and long-term trend of TCO over the TP remains unclear. Based on TOMS TCO observations, Zou (1996) estimated a decline in TCO over the TP of -0.79 ± 0.82 DU per year during the period 1978–1991. Ye and Xu (2003) also pointed out that the TCO at latitudes of the TP shows an evident decline from 1979 to 2000. However, Liu et al. (2001) used a 2-D chemistry model to simulate the ozone trend over the TP and found that the ozone above the TP was projected to recover after 1995. With the availability of TCO observations for a longer period, it is worth re-examining the long-term trend of TCO over the TP. In this paper, we use TOMS/SBUV merged TCO data and the assimilated TCO data generated by National Institute of Water and Atmospheric Research (NIWA) as well as the Whole Atmosphere Community Climate Model, version 3 (WACCM3) to analyse decadal variations of ozone and its long-term trends over the TP, and then compare them with those over the other regions at the same latitude of the TP (hereafter, 'non-TP', unless otherwise stated).

2. Data description and methods

The primary ozone data used in this study is monthly mean TOMS/SBUV merged TCO data from 1979 to 2009 (http://acdb-ext.gsfc.nasa.gov/Data_services/merged/) which is available at a horizontal resolution of 5° latitude $\times 10°$ longitude. The NIWA assimilated ozone column data, which has a horizontal resolution of 1° latitude $\times 1.25°$ longitude and covers the time period from January in 1979 to November in 2009, is also employed. More details about the NIWA data can be found in Bodeker et al. (2005). To investigate vertical variations of the ozone over the TP,

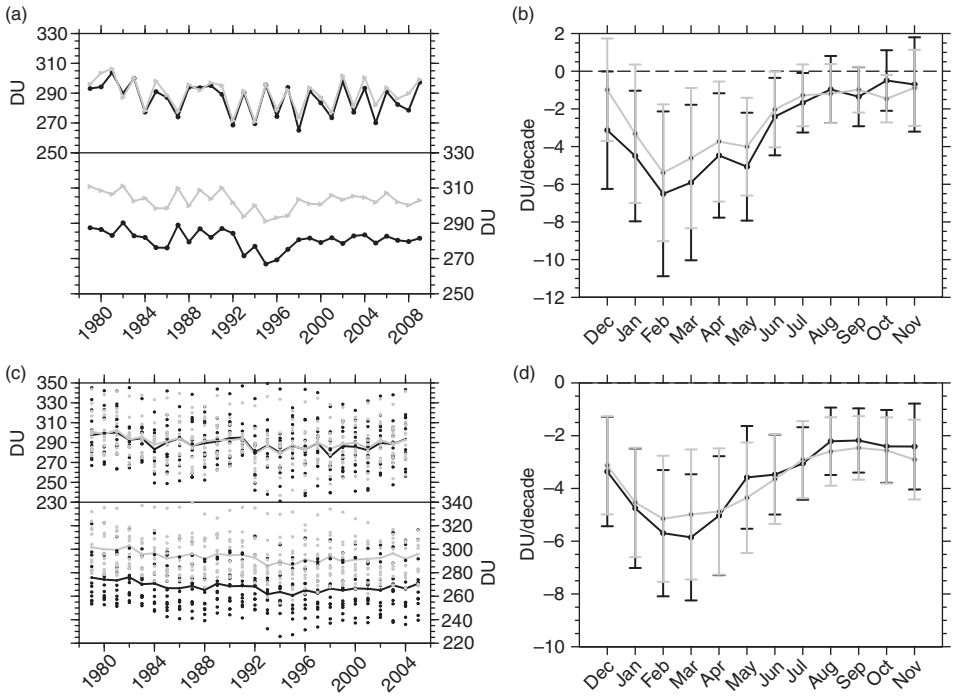

Fig. 1. (a) Time series of (top) DJF mean and (bottom) JJA mean TOMS/SBUV TCO over (black) the TP and (grey) the non-TP regions at the same latitude of the TP. (b) Seasonal variations of linear trends of monthly mean TOMS/SBUV TCO over (black) the TP and (grey) the non-TP regions for the period 1979–2009. The error bars represent uncertainties of ozone trends under a 90% confidence level. (c) The multi-model mean TCO time series averaged over all 12 CCMVal2 simulations for the period 1979–2005 (see text for details) over (black) the TP and (grey) the non-TP regions. The black and grey dots represent the corresponding values from each simulation. (d) is the same as (b), but for TCO trends derived from multi-model mean of 12 simulations for the period 1979–2005.

monthly mean ozone profiles derived from ERA-Interim reanalysis data (http://www.ecmwf.int) and the Stratospheric Aerosol and Gas Experiment II (SAGE II) dataset (ftp://ftp-rab.larc.nasa.gov/pub/sage2/v6.20) are used. The ERA-Interim ozone data spans the time period 1979–2009 and covers an altitude range from 300 to 10 hPa. Previous studies have illustrated that ERA-Interim ozone data compares well with satellite ozone observations and can be used to analyse changes in fluxes of ozone across the tropopause from 1979 to 2009 (Dragani, 2011; Skerlak et al., 2013). The SAGE II ozone data is only available for 1985–2004 and covers an altitude range of 15–40 km. The monthly surface temperature observations over the TP from the China Meteorological Administration (CMA) and the surface temperatures over the Northern Hemisphere for the period 1979–2009 from the Climatic Research Unit (CRU) TS 3.10 datasets (http://badc.nerc.ac.uk/view/ badc.nerc.ac.uk__ATOM__ dataent_1256223773328276) are also used. The 3-D wind fields and the tropopause pressure are derived from the monthly ERA-Interim data for the period 1979–2009 which has a resolution of 1.5° latitude × 1.5° longitude.

For the purpose of understanding the impact of chemical processes on ozone variations over the TP, the Whole Atmosphere Community Climate Model, version 3 (WACCM3) with 66 vertical levels from the surface to approximately 145 km is also employed. The WACCM3 has been extensively evaluated against various satellite data sets and has a good representation of stratospheric chemistry and dynamics (SPARC CCMVal 2010). The details of the model can be found in Garcia et al. (2007). Three time-slice simulations presented in this paper were performed at a resolution of 1.9° latitude × 2.5° longitude, with interactive chemistry enabled. The sea surface temperatures, greenhouse gas values, mixing ratio lower boundary conditions of CFCs and N_2O used in the control experiment (R1) are monthly mean climatology for the time period 1981–2005. The surface emissions of NOx ($NOx = NO + NO_2$) in WACCM3 are representative of those in the early 1990s (Horowitz et al., 2003). In the experiment R2 and R3,

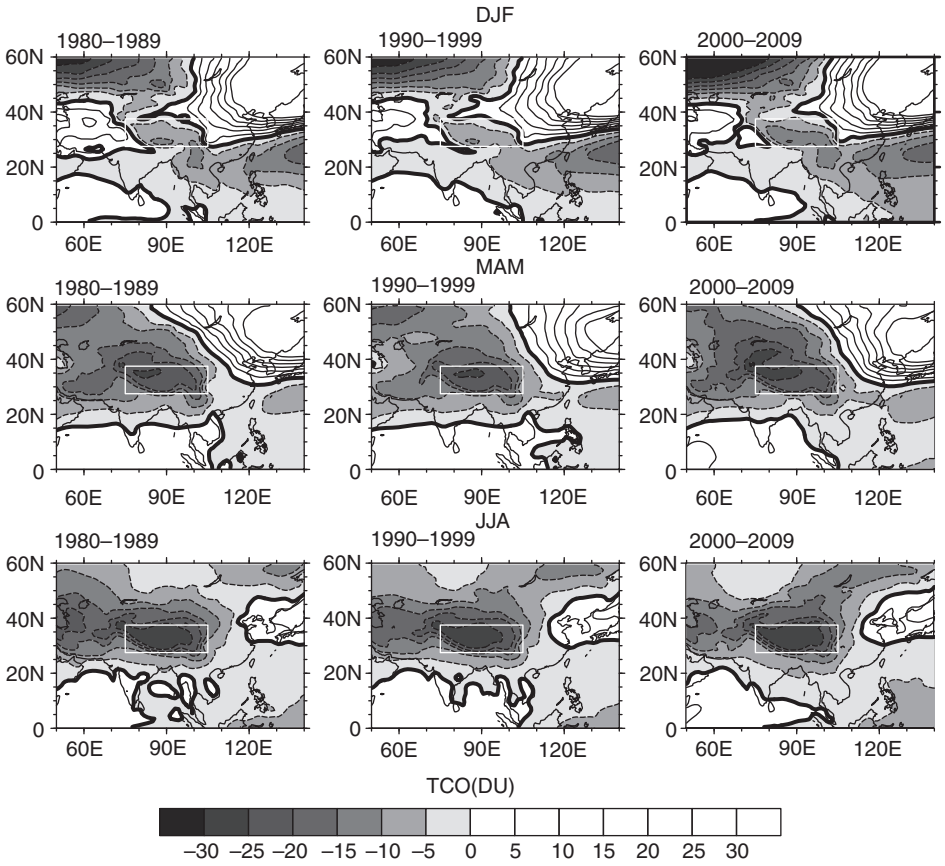

Fig. 2. Decadal mean TCO departures from the zonal mean in winter (DJF), spring (MAM) and summer (JJA) for the periods 1980–1989, 1990–1999 and 2000–2009 derived from NIWA assimilated TCO data set. The contour interval is 5 DU. Positive and negative contours are presented by the solid and dashed lines, respectively. The white rectangles represent the TP region.

all configurations are the same as R1, except that the NOx emissions in East Asia (0–90°N, 90–140°E) and the lower boundary conditions of global N_2O mixing ratio are increased by 50% and 20%, respectively. All of these three experiments were run for 25 yr with the first 5 yr excluded for the model 'spin-up' and the remaining 20 yr of data are used for the analysis.

3. Long-term trends of TCO over the TP

Figure 1a shows long-term variations of December–January–February (DJF) mean and June–July–August (JJA) mean TOMS/SBUV TCO data averaged over the TP (27.5–37.5°N, 75–105°E). The corresponding TCO values averaged over the non-TP are also shown for comparison. Consistent with the results in the earlier studies (e.g. Ye and Xu, 2003; Tian et al., 2008), the DJF mean TCO over the TP is close to that over the non-TP, while in boreal summer, the TCO over the TP is up to 20 DU lower than that over the non-TP. In phase with the global ozone trend (e.g. Angell and Free, 2009; Krzyścin et al., 2012), the annual mean TCO over the latitude of the TP shows an evident decline from 1979 to the mid-1990s and begins to recover thereafter (not shown). The recovery signal in the annual mean TCO over the TP for the period 1995–2009, at a rate of 4.71 ± 3.97 DU/decade (within 2σ confidence), is insignificantly weaker than that over the non-TP, which is about 5.84 ± 3.79 DU/decade (within 2σ confidence). Figure 1b shows the seasonal variations of TCO trends over the TP and the non-TP from 1979 to 2009. It is evident that the decline trends of the TCO over the TP are stronger than those over the non-TP during boreal winter and spring, while during summer and fall, the trends of TCO both over the TP and the non-TP are weak and close to each other. To investigate whether these results are also captured in the most recent CCM simulations, 12 CCM simulations for the period 1979–2005, performed as part of the second Chemistry–Climate Model Validation Activity (CCMVal2) (SPARC CCMVal, 2010), are also analysed. The CCMVal2 model data used in this study are from CCMVal-2 REF-B1 simulations. Detailed information about REF-B1 simulations can be found in the SPARC CCMVal (2010) report. Figure 1c shows the multi-model mean TCO time series averaged over all 12 CCMVal2 simulations. Note that the observed summertime 'ozone valley' is also visible in multi-model mean TCO time series. The multi-model mean TCO over the TP shows an overall decline before mid-1990s and a weak recovery signal afterwards, which is consistent with TCO trends from TOMS ozone data (Fig. 1a). Figure 1d further shows the modelled

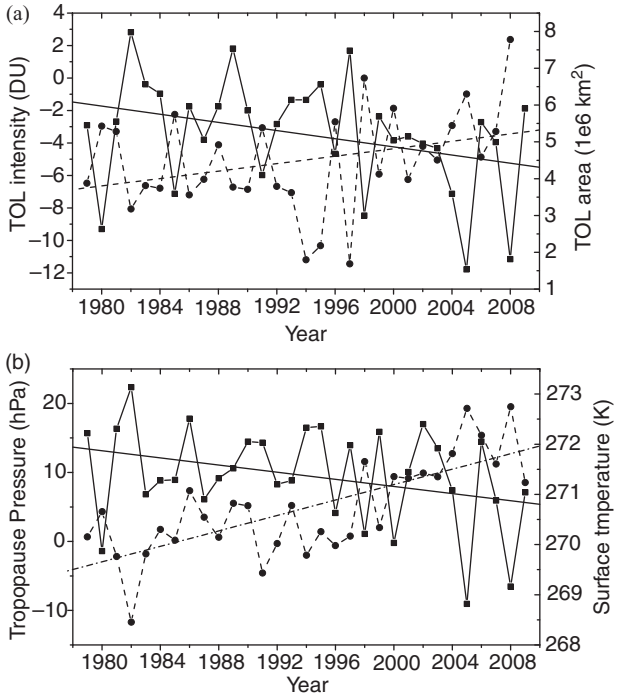

Fig. 3. (a) Time series of (solid line, left axis) DJF mean TOL intensity and (dashed line, right axis) DJF mean TOL area over the TP for the period 1979–2009. (b) Time series of (solid line, left axis) dynamic tropopause pressure differences over the TP from the non-TP regions and (dashed line, right axis) the surface temperature over the TP. The lines in (a) and (b) represent the corresponding linear trends with a 90% confidence interval of the time series for the period 1979–2009.

seasonal TCO trends over the TP. The modelled TCO trends also show a stronger decline over the TP than non-TP during winter and spring. However, differences between TCO trends over the TP and non-TP during December and January are weaker in CCMs simulations than in observations. The analysis reveals that the modelled warming trend over the TP during winter, which is an important factor influencing the TCO trend over the TP as will be discussed below, is weaker than the observed warming trend (not shown). This may be one of possible reasons why differences between TCO trends over the TP and non-TP are smaller in CCMs simulations than in observations.

Figure 2 shows the decadal variations of TCO anomalies (defined as the departure of TCO at a given location from its corresponding zonal mean) for the periods 1980–1989, 1990–1999 and 2000–2009. As expected, the summertime 'ozone valley' is the most evident. However, there exists a total column ozone low (TOL) over the TP throughout a year, that is, the TCO over the TP is always lower than that over other regions at the same latitude of the TP. Particularly noticeable is that the TOL is deepening and the area of TOL is widening during winter and spring for the period 2000–2009 than before. In contrast, the intensity and the area of the summertime TOL have no significant changes during the last three decades. To quantify the trend of TOL area in winter, the area with DJF mean TCO anomalies over the TP within the region 20.5°N-44.5°N and 70°E-110°E lower than -5 DU is counted based on the high resolution NIWA TCO data. In addition, the area-weighted average of DJF mean TCO anomalies over the TP is used as the measure of the TOL intensity. The time series of wintertime TOL area and intensity are shown in Fig. 3a. The TOL area exhibits a statistically significant positive trend of 50,000 km^2/decade while the TOL intensity has an evident negative trend of -1.4 DU/decade, indicating that the TOL area is widening and deepening. Both of these trends are statistically significant at 90% confidence level. It is also noteworthy that 2000–2009 is the period when the TOL deepens and extends at a more rapid rate than before, in accordance with Fig. 2.

4. Factors affecting the TOL trend

In this section, we will clarify the factors and processes responsible for the deepening of the TOL. Figure 3b shows dynamic tropopause pressure differences between the TP and non-TP during winter from 1979 to 2009. The dynamical tropopause is defined as the 3.5 potential vorticity unit (PVU, 1 PVU $= 10^{-6}\,K\cdot m^2\cdot s^{-1}\cdot kg^{-1}$) surface. It is evident that tropopause pressure differences between the TP and non-TP exhibit a negative trend, indicating that the wintertime tropopause height over the TP increases at a larger rate than that over the non-TP. Previous studies have showed that tropopause variations have a large impact on the TCO over the TP and lifting of tropopause height can gives rise to decreases in TCO (e.g. Varotsos et al., 2004; Tian et al., 2008). The more significant lifting of the tropopause over the TP can lead to larger TCO decreases over the TP than over non-TP. Figure 3b also indicates that the tropopause pressure differences between the TP and non-TP positively correlate with the TOL intensity with a statistically significant correlation coefficient of 0.75. The lifting of the tropopause height over the TP is closely related to the regional climate warming over the TP. Previous studies documented that the TP has warmed most rapidly in the Northern Hemisphere since the latter half of the 20th century and the largest warming rates occur during the winter months (e.g. Qin et al., 2009; Rangwala et al., 2009). Figure 3b indicates that the surface temperature over the TP exhibits

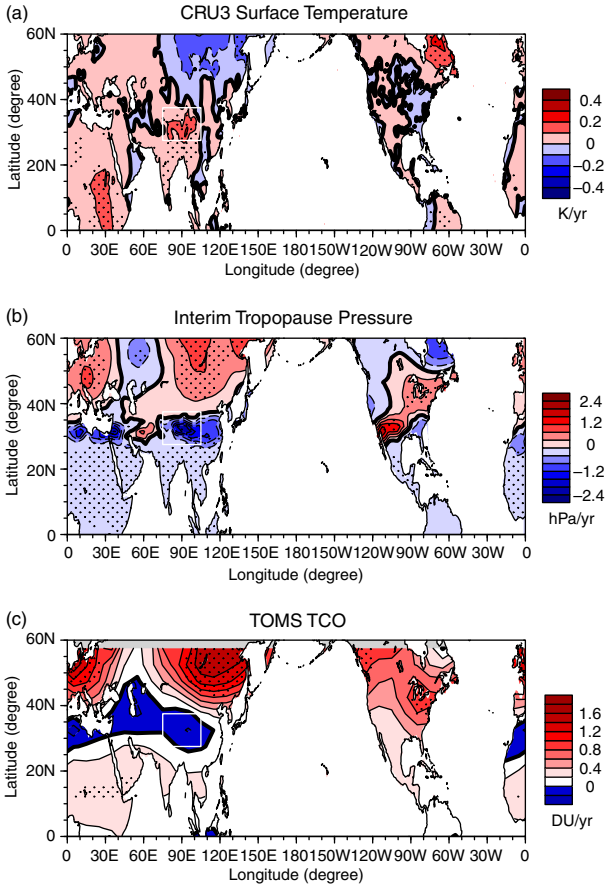

Fig. 4. (a) Linear trends of DJF mean of CRU surface temperatures over the Northern Hemisphere for the period 1990–2009. (b) Trends of thermal tropopause pressure over the Northern Hemisphere for period 1990–2009. (c) TCO trends over the Northern Hemisphere for the period 1990–2009. The dot area represents statistical significance with a 90% confidence and trends over oceans are not shown. The white rectangle in the figures represents the TP region.

an evident warming trend in winter and this warming trend becomes more significant during the period 2000–2009.

Figure 4a shows trends of DJF mean surface temperatures over the Northern Hemisphere for the period 1990–2009. Note that the TP is one of the regions in the Northern Hemisphere with a rapid and significant warming trend during this period, whereas the other regions exhibit rather weak warming, even significant cooling over the northern Eurasia and North America, which has also been reported by Cohen et al. (2012). The DJF mean of thermal tropopause pressure for the period 1990–2009 in Fig. 4b shows a significant negative trend over the TP, indicating that the tropopause over the TP is rising. Overall, Fig. 4a and b indicate that the regions with significant surface warming (cooling) are accompanied by the tropopause height increases (decreases). Figure 4c shows the linear trends of DJF mean TCO over the Northern Hemisphere for the period 1990–2009. Consistent with the results in previous studies (e.g. Krzyścin et al., 2012), the TCO in the middle and high latitudes shows significant recovery signals during this period due to the decline of ODSs, whereas the TCO in the lower latitude exhibits weaker positive trend and even negative trend, as an indication of increased tropical upwelling (Austin et al., 2010). It is particularly noticeable that the TCO over the TP exhibits a decline trend for the period 1990–2009, in accordance with the deepening of the TOL over the recent decade shown in Fig. 3a.

To further verify that the changes in TCO and tropopause pressure over the TP are both linked to the climate warming of the TP, a composite analysis is performed with respect to the DJF mean surface temperatures over the TP. Here, the warm (cold) composite for a given field is calculated by averaging the field over the years in which the DJF mean surface temperature anomaly over the TP (relative to the 1979–2009 mean annual cycle) is greater (less) than 1 (-1) standard deviation of the time series of the surface temperature for the period 1979–2009. Figure 5a shows the differences between the warm and cold composites of TCO anomalies. Note that the composited differences in TCO anomalies can be up to –10 DU, suggesting that warmer surface temperatures over the TP correspond to lower TCO values and increasing surface temperatures over the TP are responsible for the deepening of the TOL. It is worth pointing out that the surface temperature increases over the TP is not a result of decreases in TCO. Although ozone decreases over the TP will allow more ultraviolet radiation reaching the surface,

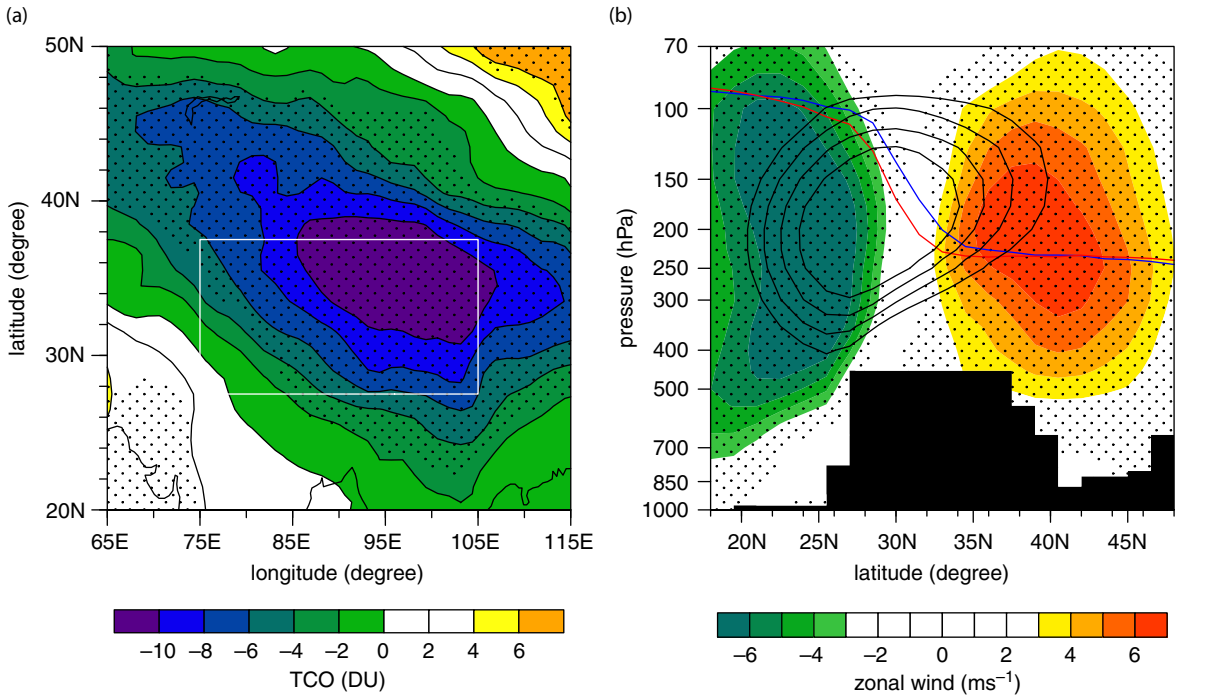

Fig. 5. (a) Differences between the warm and cold composites of DJF mean TCO anomalies (see text for more details). (b) Differences between the warm and cold composites of the zonal wind along 90°E. The composited dynamical tropopause under (blue) warm and (red) cold surface temperatures as well as climate mean (from 1979 to 2009) westerly jet (zonal winds greater than 30 m s^{-1} represented by black contours with 5 m s^{-1} interval) over the TP are also shown in (b) for reference. The dot areas in (a) and (b) represents statistical significance with a 95% confidence. The white rectangle in (a) represents the TP region and the filled dark black area in (b) represents the orography of the TP.

this energy change is too small to cause a significant warming over the TP (Forster and Shine, 1997; McFarlane, 2008). Rangwala et al. (2009) pointed out that the rapid rising of the surface temperature over the TP is directly caused by increasing downward long wave radiation due to increases in the surface humidity and absorbed solar energy when snow cover over the TP is reduced.

The wintertime warming can lead to an increase in the tropopause height over the TP not only through the expansion of air, but also via changing the jet position in the subtropics. Figure 5b shows the differences between the warm and cold composites of the zonal wind along 90°E. The composited dynamical tropopause pressures corresponding to warm and cold surface temperatures are also overplotted for reference. It is apparent that the dynamic tropopause height under anomalously warm surface temperatures over the TP is higher than that under anomalously cold surface temperatures. The zonal wind differences between its warm and cold composites show significant positive anomalies to the north of the TP and negative anomalies to the south of the TP in the upper troposphere. Compared to the climatological mean position of the westerly jet shown in Fig. 5b, these zonal wind anomalies suggest a poleward shift of the westerly jet under anomalously high temperatures over the TP, which should also contribute to the increases in the tropopause height over the TP (e.g. Liu et al., 2010; Fu and Lin, 2011).

Tian et al. (2008) argued that lifting of the tropopause height over the TP tends to cause an overall upward shift of ozone profiles, and hence reduced TCO values. Figure 6a shows the decadal mean ozone profiles over the TP for the periods 1990–1999 and 2000–2009. In the upper troposphere and lower stratosphere (UTLS), the mean ozone profile during the 2000s indeed shifts upward relative to that during the 1990s. Meanwhile, both ERA-Interim and SAGE II ozone data indicates that the negative differences of ozone mixing ratios in the UTLS over the TP from the non-TP for the time period 2000–2009 are stronger than those for the time period 1990–1999 (Fig. 6b). It can be estimated from the ERA-Interim ozone data that the larger ozone decreases between 200 hPa and 70 hPa over the TP relative to those over the non-TP in the recent decade have a 55% contribution to the deepening of the TOL.

Another factor that is likely to affect the TCO over the TP is the transport process. Austin et al. (2010) pointed out that strengthening Brewer-Dobson (BD) circulation in a warming climate can lead to ozone decreases in tropical lower stratosphere as a result of intensified upward transport of ozone-poor air from below. On the contrary, previous studies have shown convincing evidence that the Hadley circulation is strengthening in recent years (Mitas and Clement, 2005; Hu et al., 2011); consequently, the meridional transport of air mass tends to be enhanced in the UTLS at lower latitudes. Figure 6c shows meridional circulation changes between the time periods 2000–2009 and 1990–1999. The anomalous circulation shows that the meridional transport of ozone poor air in the tropical upper troposphere towards the subtropical lower stratosphere is enhanced in the 2000s and this feature is particularly pronounced above 300 hPa in subtropical UTLS. The above analysis indicate that the TCO decreases over the TP in the recent decade result mainly from the combined effect of rising tropopause and enhanced meridional transport of air masses.

To further clarify the relative importance of different factors in modulating the interannual variations of TCO over the TP, the multiple regression model (MLR) analysis is applied on the TCO time series from 1979 to 2009. The MLR is a useful tool to attribute ozone variations to dynamical, radiative and chemical effects (e.g. SPARC CCMVal, 2010; WMO, 2011). The proxy variables used here are similar to those in Dhomse et al. (2006) with the surface temperature over the TP as an additional proxy variable. The MLR can be represented as follows:

$$\begin{aligned}\mathrm{TCO}(t) = &\sum_{m=1}^{12} \alpha_m^0 \cdot \delta_{mn} + \sum_{m=1}^{12} \alpha_m^{\mathrm{EESC}} \cdot \delta_{mn} \cdot \mathrm{EESC}(t) \\ &+ \sum_{m=1}^{12} \alpha_m^{\mathrm{QBO10}} \cdot \delta_{mn} \cdot \mathrm{QBO10}(t) \\ &+ \sum_{m=1}^{12} \alpha_m^{\mathrm{QBO30}} \cdot \delta_{mn} \cdot \mathrm{QBO30}(t) \\ &+ \sum_{m=1}^{12} \alpha_m^{\mathrm{aero}} \cdot \delta_{mn} \cdot \mathrm{aero}(t) \\ &+ \sum_{m=1}^{12} \alpha_m^{\mathrm{solar}} \cdot \delta_{mn} \cdot \mathrm{solar}(t) \\ &+ \sum_{m=1}^{12} \alpha_m^{\mathrm{ENSO}} \cdot \delta_{mn} \cdot \mathrm{ENSO}(t) \\ &+ \sum_{m=1}^{12} \alpha_m^{\mathrm{EPflux}} \cdot \delta_{mn} \cdot \mathrm{EPflux}(t) \\ &+ \sum_{m=1}^{12} \alpha_m^{\mathrm{ts}} \cdot \delta_{mn} \cdot \mathrm{ts}(t) + \varepsilon(t)\end{aligned}$$

where t is the time in 1-month increments. α_m^0 ($m = 1,\ldots,12$) is the long-term mean for the mth month of the year. α_m^x is the contribution coefficient of proxy x. The proxies selected for the MLR model include the equivalent effective stratospheric chlorine (EESC), the Quasi-biennial oscillation (QBO) index at 10 and 30 hPa measured at Singapore (QBO10 and QBO30), the stratospheric aerosol 550 nm optical depths (aero), the solar cycle effect represented by F10.7 solar flux (solar), Niño3 ENSO Index (ENSO), the horizontal EP flux at 100 hPa over the 45°N to 75°N (EPflux), and the surface temperature over the TP (Ts).

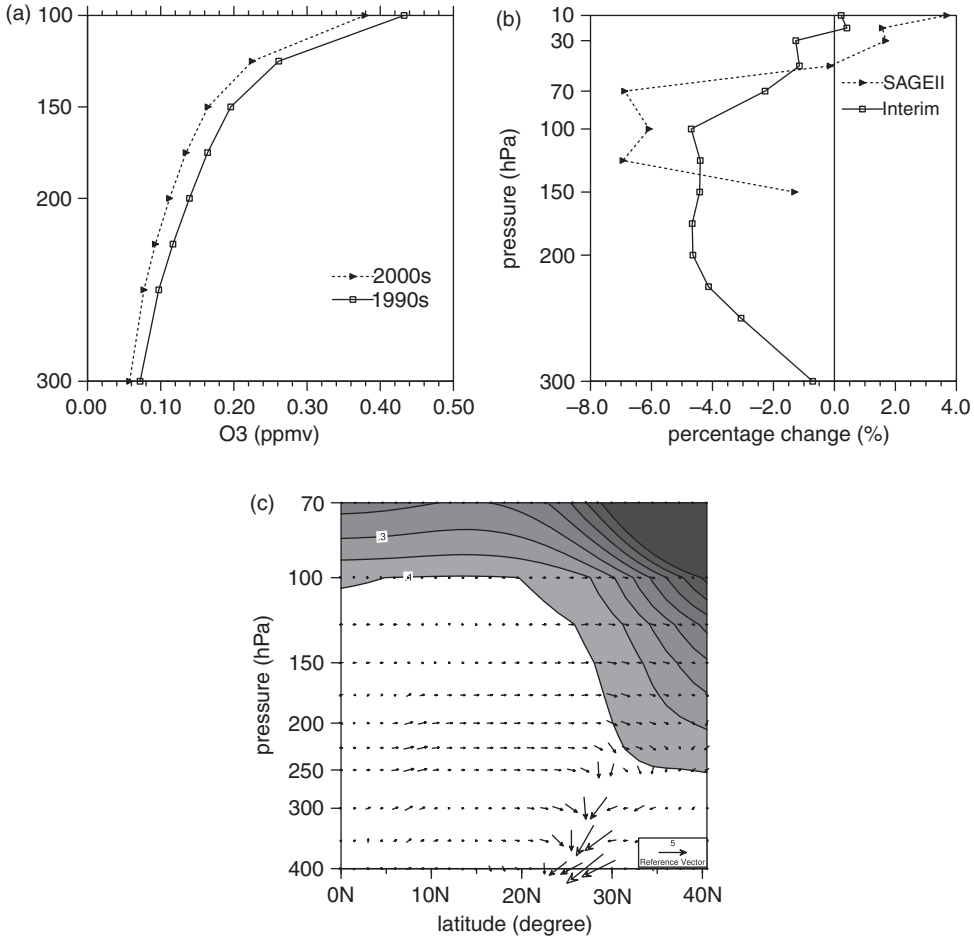

Fig. 6. (a) The decadal mean ozone profiles over the TP for the periods (solid line) 1990–1999 and (dashed line) 2000–2009. (b) Percentage differences in DJF mean of ozone differences over the TP from the non-TP between the periods 2000–2009 and 1990–1999 derived from (solid line) ERA-Interim and (dashed line) SAGE II ozone data. (c) Latitude–height cross-section of anomalous meridional circulation along 90°E between the time periods 2000–2009 and 1990–1999 (vectors in scales of 1 m s^{-1} for the meridional wind and 2 cm s^{-1} for the vertical velocity).

δ_{mn} equals 1 when index t represents one of the months of a given year and otherwise zero. $\varepsilon(t)$ represents the residual time series that generally possesses autocorrelation and contaminates the assumption in the least-squares fitting by data with random noise.

Figure 7 shows the regressed DJF mean TCO time series over the TP and the ozone variations due to EESC, solar variations, ENSO and surface temperatures over the TP. Ozone variations associated with other proxies in the MLR exhibit no significant trends and are not shown here. Note that the regressed TCO time series shows a good consistence with the observed values and the correlation coefficient between regressed and observed TCO time series is 0.89, implying that the MLR model is reliable. As expected, the ozone trend over the TP is mainly controlled by EESC variations, i.e. the declining trend in ozone before the mid-1990s and a slight recovery afterwards are in good anti-phases with EESC variations. The maximum TCO change over the TP regions caused by EESC variations can reach −7 DU during winter. It is apparent that ENSO events have no evident impacts on the ozone trend over the TP although they can cause interannual TCO variations over the TP. Figure 7 further confirms that the surface temperature changes over the TP contribute to the declining trend of the TCO in the recent decade. It is noteworthy that solar variations have an evident impact on the short-term TCO trends. During 1995–2009, the solar cycle minimum dominates and TCO decreases over the TP, resulting in a weaker recovery signal of the TCO over the TP during this period.

The above analysis suggests that the TCO decreases due to the thermal–dynamical effect of the TP during 1995–2009 offset the ozone increases due to EESC decreases. Meanwhile, the solar variations during 1995–2009 further enlarge ozone decreases over the TP in the recent decade.

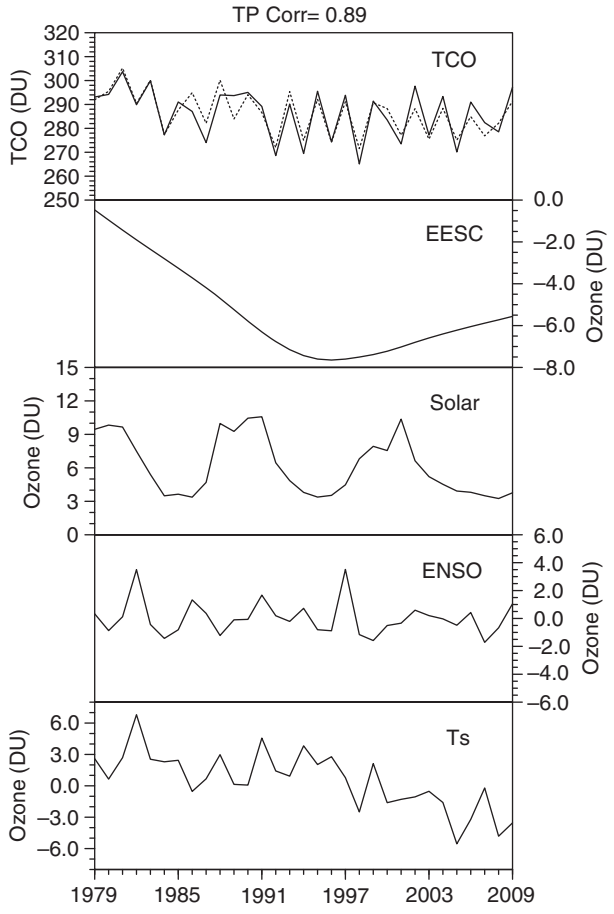

Fig. 7. Regressed (dashed line) and observed (solid line) DJF mean TCO time series over the TP. The ozone changes contributed from EESC, solar cycle, ENSO and the surface temperature are shown in unit of DU. Abbreviation 'Corr' shown in the top of the plot represents the correlation coefficient between the observed TCO and regressed TCO over the TP during winter.

The total decrease of the TCO over the TP from 1979 to 2009 is estimated to be 12 DU according to its linear trend of -0.41 DU/yr. It can be estimated from the MLR that there is a 6 DU TCO reduction due to the warming of the surface temperature over the TP from 1979 to 2009. Namely, the changes in the surface temperatures over the TP from 1979 to 2009 account for more than 50% of TCO decline in this region.

At this stage, it is necessary to further clarify whether other non-halogen containing ODSs also contribute to the deepening of the TOL over the TP. The increasing trends of the TOL area and intensity are opposite to the decline in EESC since the mid-1990s. However, it was reported that NOx ($NOx = NO + NO_2$) emissions in China have rapidly increased since the past decade with an approximately 70% increase from 1995 to 2004 (Zhang et al., 2007). In addition, the concentration of N_2O has increased by almost 20% globally since 1800 and N_2O is becoming one of the dominant ODSs in the future atmosphere (Ravishankara et al., 2009; Wuebbles, 2009). Therefore, it is worth investigating the impact of increasing NOx and N_2O on the TOL over the TP during winter.

Three WACCM simulations with and without NOx or N_2O increases were performed in this study to clarify the effect of increased NOx emissions and tropospheric N_2O mixing ratio on the TOL over the TP (see Section 2 for details). Figure 8a and b show the vertical distribution of ozone differences over the TP between WACCM control run R1 and sensitivity runs R2 and R3. In contrast to ozone decreases in the UTLS in the ERA-Interim and SAGE II ozone profiles in 2000s as shown in Fig. 6b, a 50% NOx increase in East Asia causes a 2% increase in ozone mixing ratios in the UTLS from 70 to 200 hPa. Due to its short chemical lifetime (Browne and Cohen, 2012), NOx are mostly destroyed in the troposphere and an increase in NOx emissions at the surface has rather small effects on NOx concentrations in the stratosphere. In the troposphere, NOx increases in East Asia can only yield more ozone via photochemical reactions. Consequently, a 50% increase in NOx emissions in East Asia causes a statistically significant TCO increase over the southern part of the TP and a slight TCO decrease to the north of the TP (Fig. 8c). This spatial difference in TCO changes over different part of the TP may be related to stronger ultraviolet irradiance and higher water vapour abundance in the troposphere over the southern TP than over the northern TP.

In run R3 in which N_2O is globally increased by 20% relative to that in control run R1, there is a significant ozone decrease of 5% in the lower and middle stratosphere (70–10 hPa) compared to control run R1 (Fig. 8b). This is understandable since more N_2O can give rise to more ozone loss through NOx-induced ozone destruction in the middle stratosphere (e.g. Portmann et al., 2012). It is likely that the ozone increase in the upper troposphere is a self-healing response to the ozone loss higher up, whereby ozone production is enhanced by the increased UV available under stratospheric ozone depletion. It is worth noting that there are no significant increases in tropospheric NOx and ozone in R3 as compared to R1. Figure 8d shows the TCO differences between run R3 and R1. It is clear that the TCO over the whole TP decreases when N_2O is increased by 20%. In the R2, the 50% increase of NOx emissions in East Asia yields a TCO increase of about 1 DU, whereas a global 20% N_2O increase in run R3 causes a TCO decrease of about 3 DU, implying the net TCO decreases are no more than 2 DU. This result implies that the increases of NOx emissions and tropospheric N_2O mixing ratio from 1979 to 2009 account for no more than 20% reductions in TCO over the TP. However, it is worth pointing out that NOx

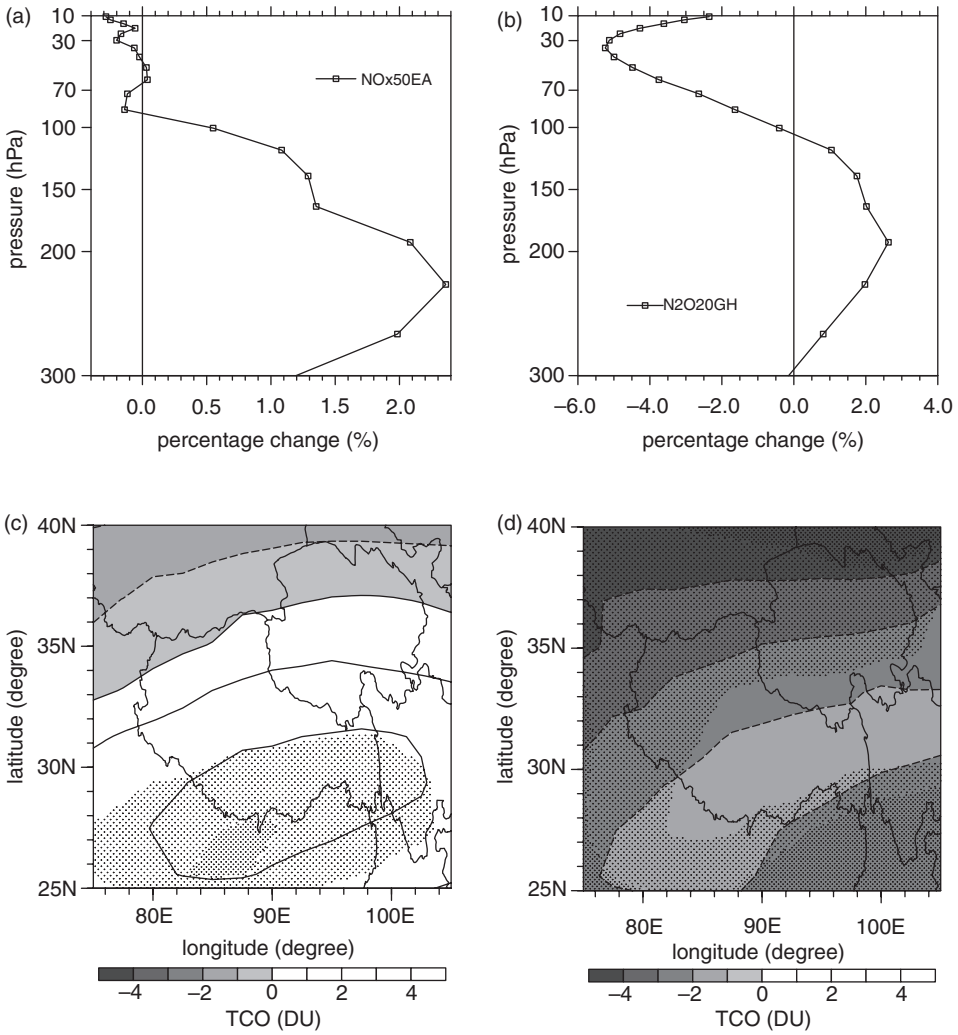

Fig. 8. (a) Percentage differences in DJF mean of ozone over the TP between runs R1 and R2. (b) is the same as (a), but for ozone differences between R1 and R3. (c) DJF mean of TCO differences between R1 and R2. (d) is the same as (c), but for TCO differences between R1 and R3. The dot areas in (c) and (d) represent statistical significance with a 90% confidence.

increases in East Asia in the future might offset the negative TCO trend over the TP.

5. Conclusions

Using various observations and a chemistry–climate model, the long-term trends of TCO over the TP and factors responsible for these trends are analysed in this study. The analysis reveals that the TOL over the TP during winter and spring is deepening, especially within the period 2000–2009, although annual mean TCO over the TP begins to recover since the mid-1990s. The TOL intensity in winter is increasing at a rate of 1.4 DU per decade and the TOL area is extending with 50,000 km^2 per decade. The deepening of the TOL also leads to a slower recovery signal in annual mean TCO over the TP than that over the non-TP regions at the same latitudes.

The TP is characterised by significant and rapid surface warming during winter for the period 1990–2009. Increasing surface temperatures over the TP make a large contribution to the deepening of the TOL in boreal winter and spring and the rapid warming of the TP in the 2000s corresponds to the stronger deepening of the TOL. The warming of the TP and associated poleward shift of the westerly jet lead to a lifted tropopause over the TP and cause a reduction in TCO. In addition, enhanced meridional transport of ozone-poor air in tropical upper troposphere towards the subtropical lower stratosphere also gives rise to ozone decreases in the UTLS over the TP and makes a contribution to the deepening of the TOL.

Based on the MLR analysis, the TCO trends over TP are mainly controlled by EESC and are evidently affected by the surface warming of the TP and solar variations. The ozone reductions due to rising surface temperature cause a weaker recovery signal of TCO over the TP in the recent decade compared to that over the non-TP, while solar cycle minimum makes the ozone recovery signal even weaker after mid-1990s. Rising surface temperatures over the TP for the period 1979–2009 account for up to 50% of TCO decline over the TP, while increases in NOx emissions and tropospheric N_2O contribute to no more than 20% reductions in TCO for the period 1979–2009.

The deepening of the TOL makes the recovery of TCO over the TP less significant than that over the non-TP regions of the same latitudes. Rangwala et al. (2010) have shown that the surface temperature over the TP during winter and spring will continue to rise at a rapid rate during the 21st century under the SRES A1B scenario. Therefore, the TOL over the TP during winter and spring is likely to deepen and extend continuously. In addition, the increasing global tropospheric N_2O in the future might further deepen the TOL over the TP. However, for the foreseeable future, the impact of global warming/loss of snow over the TP on the TOL will be mitigated by decreasing chlorine and bromine loading in the stratosphere and NOx emissions increases in East Asia.

6. Acknowledgements

This work is supported by the National Science Foundation of China (41175042, 41225018) J. Luo is supported by the Scholarship Award for Excellent Doctoral Student granted by Lanzhou University. The authors thank the scientific teams NASA, ECMWF, CRU and China Meteorological Administration for providing data. Dr. Greg Bodeker kindly provided the NIWA TCO data. Comments and suggestions from the anonymous reviewers and the editor were valuable in improving the quality of this paper. The authors also thank Dr. Eri Saikawa, Prof. Aijun Ding and Dr. Dong Guo for their helpful suggestions. Finally, the authors acknowledged the computing support provided by the Supercomputing Center of Cold and Arid Regions Environmental and Engineering Research Institute of Chinese Academy of Sciences.

References

Angell, J. K. and Free, M. 2009. Ground-based observations of the slowdown in ozone decline and onset of ozone increase. *J. Geophys. Res.* **114**, D07303, 1–9.

Austin, J., Scinocca, J., Plummer, D., Oman, L., Waugh, D. and co-authors. 2010. Decline and recovery of total column ozone using a multimodel time series analysis. *J. Geophys. Res.* **115**, D00M10.

Bodeker, G. E., Shiona, H. and Eskes, H. 2005. Indicators of Antarctic ozone depletion. *Atmos. Chem. Phys.* **5**, 2603–2615.

Browne, E. C. and Cohen, R. C. 2012. Effects of biogenic nitrate chemistry on the NOx lifetime in remote continental regions. *Atmos. Chem. Phys.* **12**, 11917–11932.

Cohen, J. L., Furtado, J. C., Barlow, M., Alexeev, V. A. and Cherry, J. E. 2012. Asymmetric seasonal temperature trends. *Geophys. Res. Lett.* **39**, L04705.

Dhomse, S., Weber, M., Wohltmann, I., Rex, M. and Burrows, J. P. 2006. On the possible causes of recent increases in northern hemispheric total ozone from a statistical analysis of satellite data from 1979 to 2003. *Atmos. Chem. Phys.* **6**, 1165–1180.

Dragani, R. 2011. On the quality of the ERA-Interim ozone reanalyses: comparisons with satellite data. *Q. J. R. Meteorol. Soc.* **137**, 1312–1326.

Forster, P. M. d. F. and Shine, K. P. 1997. Radiative forcing and temperature trends from stratospheric ozone changes. *J. Geophys. Res.* **102**, 10841–10855.

Fu, Q. and Lin, P. 2011. Poleward shift of subtropical jets inferred from satellite-observed lower-stratospheric temperatures. *J. Clim.* **24**, 5597–5603.

Garcia, R. R., Marsh, D. R., Kinnison, D. E., Boville, B. A. and Sassi, F. 2007. Simulation of secular trends in the middle atmosphere, 1950–2003. *J. Geophys. Res.* **112**, D09301.

Horowitz, L. W., Walters, S., Mauzerall, D. L., Emmons, L. K., Rasch, P. J. and co-authors. 2003. A global simulation of tropospheric ozone and related tracers: description and evaluation of MOZART, version 2. *J. Geophys. Res.* **108**(D24), 4784.

Hu, Y. Y., Zhou, C. and Liu, J. P. 2011. Observational evidence for the poleward expansion of the Hadley circulation. *Adv. Atmos. Sci.* **28**(1), 33–44.

Krzyścin, J. W. 2012. Onset of the total ozone increase based on statistical analyses of global ground-based data for the period 1964–2008. *Int. J. Climatol* **32**, 240–246.

Liu, C. X., Liu, Y., Cai, Z. N., Gao, S. T., Bian, J. C. and co-authors. 2010. Dynamic formation of extreme ozone minimum events over the Tibetan Plateau during northern winters 1987–2001. *J. Geophys. Res.* **115**, D18311.

Liu, Y., Li, W. L. and Zhou, X. J. 2001. Prediction of the trend of total column ozone over the Tibetan Plateau. *Science in China.* **44**(Suppl), 385–389 (in Chinese).

McFarlane, N. 2008. Connections between stratospheric ozone and climate: radiative forcing, climate variability, and change. *Atmos. Ocean* **46**, 139–158.

Mitas, C. M. and Clement, A. 2005. Has the Hadley cell been strengthening in recent decades? *Geophys. Res. Lett.* **32**, L03809.

Portmann, R. W., Daniel, J. S. and Ravishankara, A. R. 2012. Stratospheric ozone depletion due to nitrous oxide: influences of other gases. *Phil. Trans. R. Soc. B.* **367**, 1256–1264.

Qin, J., Yang, K., Liang, S. L. and Guo, X. F. 2009. The altitudinal dependence of recent rapid warming over the Tibetan Plateau. *Clim. Change.* **97**, 321–327.

Rangwala, I., Miller, J. R., Russell, G. L. and Xu, M. 2010. Using a global climate model to evaluate the influences of water

vapour, snow cover and atmospheric aerosol on warming in the Tibetan Plateau during the twenty-first century. *Clim. Dyn.* **34**, 859–872.

Rangwala, I., Miller, J. R. and Xu, M. 2009. Warming in the Tibetan Plateau: possible influences of the changes in surface water vapor. *Geophys. Res. Lett.* **36**, L06703.

Ravishankara, A. R., Daniel, J. S. and Portmann, R. W. 2009. Nitrous oxide (N_2O): the dominant ozone-depleting substance emitted in the 21st century. *Science*. **326**, 123–125.

Skerlak, B., Sprenger, M. and Wernli, H. 2013. A global climatology of stratosphere-troposphere exchange using the ERA-interim dataset from 1979 to 2011. *Atmos. Chem. Phys. Discuss.* **13**, 11537–11595.

SPARC CCMVal. 2010. *SPARC Report on the Evaluation of Chemistry–Climate Models*. V. Eyring, T. G. Shepherd, D. W. Waugh (Eds.), SPARC Report No. 5, WCRP-132, WMO/TD-No. 1526.

Tian, W. S., Chipperfield, M. P. and Huang, Q. 2008. Effects of the Tibetan Plateau on total column ozone distribution. *Tellus B.* **60**, 622–635.

Tobo, Y., Iwasaka, Y., Zhang, D. Z., Shi, G. Y., Kim, Y. S. and co-authors. 2008. Summertime 'ozone valley' over the Tibetan Plateau derived from ozonesondes and EP/TOMS data. *Geophys. Res. Lett.* **35**, L16801.

Varotsos, C., Cartalis, C., Vlamakis, A., Tzanis, C. and Keramitsoglou, I. 2004. The long-term coupling between column ozone and tropopause properties. *J. Clim.* **17**, 3843–3854.

World Meteorological Organization (WMO). 2011. *Scientific Assessment of Ozone Depletion: 2010*. Global Ozone Research and Monitoring Project-Report No. 52, WMO, Geneva, Switzerland.

Wuebbles, D. J. 2009. Nitrous oxide: no laughing matter. *Science*. **326**(5949), 56–57.

Yanai, M., Li, C. F. and Song, Z. S. 1992. Seasonal heating of the Tibetan Plateau and its effects on the evolution of the Asian summer monsoon. *J. Meteorol. Soc. Jpn.* **70**, 319–351.

Ye, D. Z. and Wu, G. X. 1998. The role of the heat source of the Tibetan Plateau in the general circulation. *Meteorol. Atmos. Phys.* **67**, 181–198.

Ye, Z. J. and Xu, Y. F. 2003. Climate characteristics of ozone over Tibetan Plateau. *J. Geophys. Res.* **108**(D20), 4654.

Zhang, Q., Streets, D. G., He, K. B., Wang, Y. X., Richter, A. and co-authors. 2007. NOx emissions trends for China, 1995–2004: the view from the ground and the view from space. *J. Geophys. Res.* **112**, D22306.

Zheng, X. D., Zhou, X. J., Tang, J., Qin, Y. and Chan, C. Y. 2004. A meteorological analysis on a low tropospheric ozone event over Xining, North Western China on 26–27 July 1996. *Atmos. Environ.* **38**, 261–271.

Zhou, X. J., Luo, C., Li, W. L. and Shi, J. E. 1995. Ozone changes over China and low center over Tibetan Plateau. *Chin. Sci. Bull.* **40**, 1396–1398 (in Chinese).

Zou, H. 1996. Seasonal variation and trends of TOMS ozone over Tibet. *Geophys. Res. Lett.* **23**(9), 1029–1032.